IEEE Access
Multidisciplinary | Rapid Review | Open Access Journal

Received February 2, 2021, accepted February 28, 2021, date of publication March 15, 2021, date of current version March 23, 2021.

Digital Object Identifier 10.1109/ACCESS.2021.3065873

Expansion of the Fused Filament Fabrication (FFF) Process Through Wire Embedding, Automated Cutting, and Electrical Contacting

FABIAN ZIERVOGEL, LUKAS BOXBERGER, ANDRÉ BUCHT, AND WELF-GUNTRAM DROSSEL
Fraunhofer Institute for Machine Tools and Forming Technology, 01087 Dresden, Germany
Corresponding author: Lukas Boxberger (lukas.boxberger@iwu.fraunhofer.de)

ABSTRACT Additive manufacturing is establishing new forms of manufacturing processes to produce functional parts. It is thus seen as a hope for a shift towards decentralised production and the associated positive effects on the environment. The most widespread process, Fused Filament Fabrication, already impresses with a large variety of materials and the possibility of including non-polymeric additives as fibre materials. To support this development, this paper describes a form of wire implementation as an add-on for existing FFF systems, that can be realised without major changes to hardware or software. The aim is to integrate electrical functions directly into the component - in one manufacturing process. The process is based on a hybrid material made of PLA with a copper core, which was developed in advance. Within this work, two retrofittable units for FFF printers are described, which cut a continuous wire with a diameter of 0.2 *mm* embedded in a polymer in a fully automatic manner. Furthermore, two thermal contacting processes are presented, which make it possible to contact the embedded wire via the heated extruder nozzle and metallic inserts. Thereby, a best contact resistance of $0.009 \pm 0.0023\ \Omega$ (50% confidence interval) could be achieved for a screw contact. For a plug-in or solder contacts, a contact resistance of $0.059 \pm 0.028\Omega$ (50% confidence interval) was realised. In terms of process technology, the wire deposition within the plastic structure could be reliably realised at printing speeds of 10 mm/s on straight sections and 1 mm/s in curves with a radius of 5 *mm*. The developed process was successfully validated using a functional demonstrator. The functional sample can be selectively heated to the glass transition temperature and reversibly formed. In summary, the developed methods are suitable for cost-effectively expanding existing FFF systems to integrate electrical functions during the 3D printing process.

INDEX TERMS 3D-printing, additive manufacturing, automated wire placement, automated contacting, composite materials, computer aided manufacturing, contact resistance, embedded wires, generative manufacturing, hybrid filament, hybrid integrated circuits, integrated manufacturing systems, integrated circuit manufacture, thermoforming.

I. INTRODUCTION

The additive manufacturing, in the form of 3D printing, has been steadily growing in popularity since its invention in 1980 [1]. The technology makes it possible to produce end-use parts from digital models in one processing step. The most common form is the Fused Filament Fabrication (FFF) process [2], [3], which generates objects from thermoplastic polymers. Compared to Selective Laser Melting (SLM) or Multi Jet Fusion (MJF), this variant of 3D printing is currently inexpensive to purchase and maintain, as well as low barrier to set-up and post-curing. Due to the above-mentioned properties, the technology is not only used in large, but also in small and medium-sized companies. Last but not least, it is already available in some private households. This means that the process is currently predestined for the decentralised production of consumer goods like no other. And it thus has the potential to deliver considerable added value for a more climate-friendly and crisis-proof production of the future [4].

In order to tap the potential for decentralised production, the performance spectrum of FFF-based production machines and the component functions and properties that

The associate editor coordinating the review of this manuscript and approving it for publication was Yangmin Li.

can be generated must be increased. The latter can already be achieved by component hybridisation through the integration of non-polymeric fillers. By adding pre-impregnated fibres made of glass or carbon, it is already possible to produce structural components with significantly better strengths and targeted force dissipation paths [5]. To move from passive structural components to active, controllable functional components, conductive materials are introduced into the component as part of the build process. This is done by conductive pastes [6], surface deposition [7], [8], conductive polymers [9]–[11] or implemented wires [12].

- *Conductive Pastes:* Deposition can be done on both planar and non-planar surfaces. However, the materials for deposition are price-intensive, which makes it uneconomical for larger quantities. At the same time, additional machine components such as dispensers and lasers, some of which are expensive, are required for substrate preparation. If the final product is to be processed, the production machine must be FFF printable and include an additional dispenser mechanism. Finally, after deposition, a curing process of the paste is too often necessary, requiring additional process steps and machines or machine components. This post-curing process sometimes places demands on the carrier substrate that can lead to limitations in direct comparison with later product requirements.
- *Surface Deposition:* Similar to conductive pastes, the deposition can be performed three dimensional on a surface. Here are multiple possible methods, including Aerosol-Jetting, Laser Direct Structuring (LDS) or the plasmadust process. These applications all require at least one additional tool head to perform and in case of LDS further post processing. Not all thermoplastics are compatible with those methods, due to process temperatures or needed additives.
- *Conductive Polymers:* The application of conductive polymers requires a reduced machine setup. They can already be used with conventional multi-material printers, such as desktop variants with dual extruders, and can be used to create complex functional parts [11]. However, these polymers exhibit high resistivity and negative nozzle wear [9].
- *Implemented Wires:* Wire integration has the advantage of lower base material cost and greater variety of usable materials. The wires can be applied endlessly and analogous to fiber integration on already 3D printed parts or integrated directly into the part and do not require a thermal postcuring process.

Three sub-processes are required for a fully automated process within one machine:

- 1. wire deposition
- 2. cutting the continuous wire
- 3. contacting the wire within and outside of the part

Wire deposition during part creation can be accomplished by the following methods:

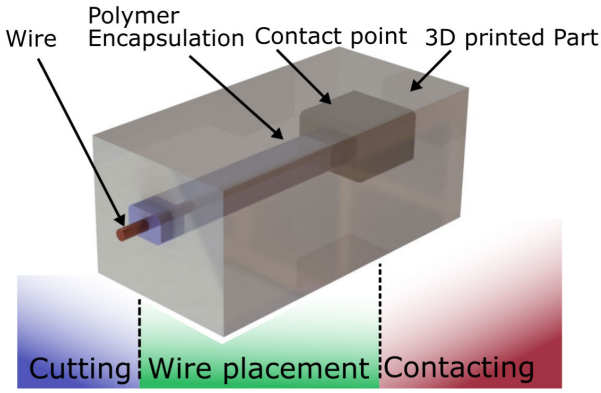

FIGURE 1. Depiction of a printed part with integrated wire and contact element. Needed technologies are displayed in different colours.

a feeding of a preimpgregnated wire, that is pressed onto the parts surface (not commercially available) [13], [14]
b separated feeding of polymer and wire into a shared heating chamber and extrusion as compound (not commercially available) [15]–[19]
c feeding the wire beneath the nozzle, wires is encapsulated by overprinting (not commercially available) [20]–[24]
d thermally pressed into the polymer substrate (commercially available) [12], [25], [26]

In all the methods shown, a wire cut is realized in the section between the contact area of substrate and wire and the feeding mechanism. The commercial implementation of the thermal pressed wire (d) takes place on a different machine, as the 3D printer. The contacting is done by automated soldering [12]. Wires with a diameter of 0.32 *mm* can be integrated. In process (c) a contacting is done by an electrical conductive polymer composite (ECPC) [21], which is extruded in the printer via an additional dispenser. Currently, wires with a diameter of 0.137 *mm* can be integrated. The processes (a), (b) do not have a form of contacting yet. One of the processes shown is realized by expanding an existing 3D-printer [17]. In the current trend of end use part production through AM, FFF is still the most applied technology and is said to made the most revenues in 2019 [3]. In view of the widespread use of FFF technology, retrofitting existing machines can be a major advantage for adaptation in the industrial, SME and private sectors. Provided that a cost-effective retrofit option can be developed and made available on the market, that is compatible regardless of manufacturer/model, and that the required settings in hardware and software are low-threshold, we see the potential for the technology to enable a high level of acceptance, widespread use, and rapid further development of the basic technology and processes.

By integrating metallic wires directly into the component, within the manufacturing process, manual work steps can be reduced, new component functions can be created and

lightweight design potential can be exploited. Depending on the wire used, actuator, sensor, signal or power conducting as well as heating functions can be embedded locally. These can be used, for example, to record local component loads, which can be used in the field of structural health monitoring, for the realization of components with inherent force measurement systems for, for example, load-sensing, individualized shoe insoles or for data acquisition and optimization of production machines. Furthermore, partial intrinsic structural heating can be used to subsequently generate targeted and repeatable component deformations that can be used in the field of structural morphing, for iterative ergonomic adaptation of tools, sporting goods and backpacks, opening/closing mechanisms or for geometric fine adjustment of orthoses, prostheses, or corsets [27]. Finally, electrical connections within the component or to neighbouring components can be realized, resulting in a wide range of lightweight construction potentials. The range of applications for the manufactured parts is thus extremely versatile and can be used across a wide range of industries.

II. MATERIALS AND METHODS

The aim of this work was to develop an extension for the FFF process that enables a printer to automatically integrate and contact wires during additive manufacturing. In order to address the wide range of users and to enable easy application, the focus was on simple implementation in printer systems. This was to be achieved by using suitable and established components and user-friendly process conditions. We used a commercially available 3D printer from the mid-price segment, the X350Pro from the manufacturer German RepRap (year of construction 2015, see Fig.2), which we updated to the open-source firmware Marlin 2.0.7.2. and modified slightly mechanically.

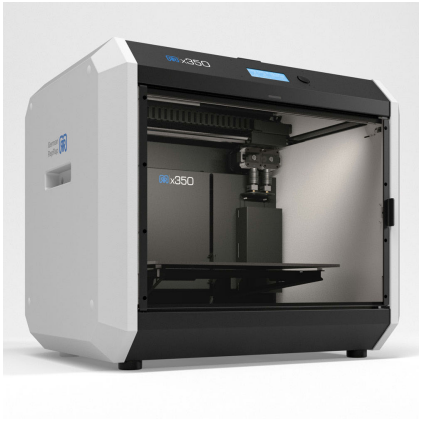

FIGURE 2. The X350 Pro FFF Printer, which was used for this research [28].

This printer has a dual extruder setup in direct drive variant as standard, which was revised for testing purposes. In these changes, the dual direct drive has been retained, but the printhead has been rebuilt to allow for more connectivity and a modular design. The hotend systems used are two V6 all-metal hotends from E3d. These hotends are the most commonly used heated components for 3D printers. The extruders from the German RepRap X350 Pro were retained. These are single-gear extruders with no gear ratio, as is common in various printers. They contain a drive gearbox that is connected to a stepper motor. This gear faces a bearing and therefore mechanically engages the filament when it is pushed forward. The notch on the drive gear that centres the filament is 0.3 *mm* deep. Therefore, the smallest usable filament size was set at a diameter of 0.4 *mm*.

The wire diameter used was kept the same in all filament samples produced in order to be able to observe the influence of the difference in wire content in the cross-section. A 0.2 *mm* thick wire was chosen in order to achieve a fibre content of less than 50%, in the thinnest filament sample. It is assumed that a higher ratio does not lead to sufficient fixation of the wire. A single wire is provided for this purpose. Stranded wires are not considered, as preliminary tests have shown that they cause problems in filament production. As part of this research, a wire integration process was developed based on a hybrid filament that was produced in a separate machine. The design details of this device will not be discussed further in this paper. The filament produced was wound onto a spool and placed in the FFF printer analogously to ''conventional'' filaments. This means that it is fed from an extruder inside the hotend, where a melt zone forms inside the heating block due to the temperatures above the melting point of the polymer used. The extruder builds up pressure which forces the molten polymer through a nozzle onto a build-up surface. To achieve automation of wire deposition, two cutting devices were developed and compared. Both implementations cut the wire below the nozzle and were mounted to the print head. The focus in the development of these modules was on the possibility of adapting the cutter module to different printing machines from different manufacturers by means of a coupling plate. This enables independent integration and use. Derived from the conditions of the delivery, two methods of contacting were developed. One method for an electrical screw contact and one for a plug-in contact. Both methods were measured with regard to contact resistance. Subsequently, a simple demonstrator was constructed, which was manufactured with the evaluated, constructive and process-specific preferred methods. In this study, the mechanical properties of the composite materials produced are not discussed, since in contrast to the embedding of carbon fibres, the focus is on the benefits of electrical conductivity. The wire embedding (A), cutting (B) and contacting (C) subsections are described in detail below.

A. WIRE EMBEDDING

- fixed parameters:
  - Matrix material: Raise3D Premium PLA Red, filament diameter 1.75 *mm*;
  - materials of the Hybrid Filament: Hybrid filament proprietary development consisting of transparent

PLA sheath (Fillamentum Crystal Clear) with a core of copper wire (CU-V 100/0.20 BLOCK);
  - wire diameter 0.2 *mm*;
  - nozzle size 0.4 *mm*;
  - printing temperature 200° C, heated bed 60° C
- varying parameters:
  - diameter of the hybrid filament;
  - speed of wire deposition;
  - radius while changing directions;
  - layer height hybrid line

For wire integration, a concept was developed that follows the concept of deposition by pre-impregnated wires (cf. (a)). A hybrid filament containing a continuous wire is produced in advance. In the hotend, the thermoplastic polymer is melted and pushed through a nozzle along the wire. Following the concept of electrically conductive polymers, the dual material structure of the printer is used to create conductive, functional parts with one hotend and the structure of the part with the other. This allows the settings and printing parameters to be set differently for each hotend. The settings used for the printed substrate were 215°C with 60 mm/s print speed at 0.2 *mm* layer height.

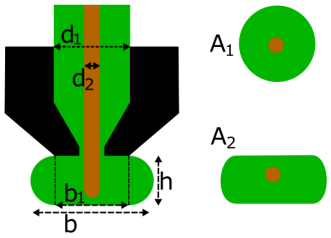

FIGURE 3. Deposition Process of the hybrid filament through a hotend (Green - Polymer; Brown - Wire; Black - Nozzle; A_1 - filament cross-section; A_2 - line cross-section; d_1 - hybrid filament diameter; d_2 - wire diameter, b_1 - sub-width; b - line width; h - layer height).

The wire is fed, bound to the polymer, and extruded. In order to extrude the wire and the polymer evenly and avoid displacement, the feed of the hybrid filament is adjusted directly proportional to the extruded path length. As a result, the cross-section of the deposited line equals that of the fed hybrid filament. This process is illustrated in Fig.3. The cross section of the hybrid filament is described in Eq.1 and Eq.2 displays the cross-section of the printed line. In order to distribute enough power for the application demonstrator of a conformable surface that is formed by taking advantage of softening over time due to resistance heating, the wire in this research was defined as a 0.2 *mm* thick copper wire. The diameter of the wire is within the order of conventional layer heights used in FFF printing and is higher as in comparable methods [12], [21], [17]. This leads to a need for higher layer heights for the hybrid paths, to enable a deflection of the wire moving direction with a certain radius. The filament diameter is a function in dependency of the line parameters b and h. By equating Eq.1 and Eq.2, regarding Eq.3, Eq.4 is recieved. Solving Eq.4 for d_1, describes the dependency of the filament diameter with Eq.5.

$$A_1 = \frac{d_1^2}{4} * \pi - \frac{d_2^2}{4} * \pi \tag{1}$$

$$A_2 = \frac{h^2}{4} * \pi + h * b_1 - \frac{d_2^2}{4} * \pi \tag{2}$$

$$b_1 = b - h \tag{3}$$

$$\frac{\pi}{4} * (d_1^2 - d_2^2) = \frac{\pi}{4} * (h^2 - d_2^2) - h^2 + h * b \tag{4}$$

$$d_1 = \sqrt{h^2 * (1 - \frac{4}{\pi}) + b * h * \frac{4}{\pi}} \tag{5}$$

From this equation the graph shown in Fig. 4 can be deduced. In order to obtain a viable combination of line parameters, these were tested analytically. Based on the observations and preliminary considerations, it was determined that the selection of a viable diameter for the hybrid filament is an optimisation problem with the following factors:

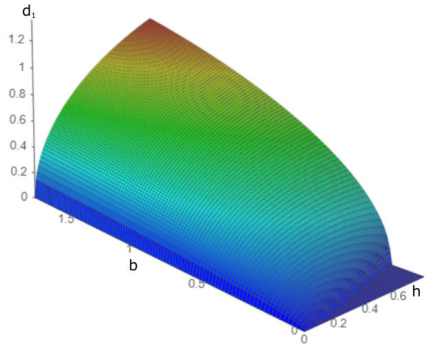

FIGURE 4. 3D plot of the usable hybrid filament diameters (d) in dependency of the width(b) and height(h) of the printed line.

- 1. Wire diameter d_2 (has to be lower, than the layer height/ line width of the hybrid path to be encapsulated)
- 2. Line width b (higher widths increase the needed space, decrease the required positioning accuracy of the deposited wire)
- 3. Layer height h (higher heights increases the needed space, increase redirection radius of the wire, increase certainty of encapsulating the wire, has to compatible with other layer heights in object)
- 4. Filament diameter d_1 (higher diameters decrease chance of filament breaks)

For further testing, different hybrid filaments with different diameters were made using polylactide (PLA). For all configurations, a clear material was chosen to assess the condition of the deposited wire. Individual line geometry parameters (b - line width; h - layer height) were chosen for each filament configuration. The layer heights were set to common layer heights or multiples thereof to achieve good compatibility between the matrix layers and the hybrid lines. The width of the line was set to 1.9 - 2.6 times the layer height to achieve fixation of the wire within curves. The configurations used and the associated parameters are shown in Tab.2.

TABLE 1. Overview on the manufactured hybrid filaments. Depiction of the characteristics, testing parameters and sample names. All with 0.2 *mm* bare copper wire, encapsulated in PLA.

filament diameter in mm	layer height in mm	line width in mm	sample name
1.2	0.75	1.43	F12
1	0.6	1.43	F10
0.75	0.4	1.05	F075
0.45	0.25	0.54	F045

TABLE 2. Overview of the printing problems that occurred and the associated causes.

Behaviour	Reason	Solution
Clogging	Lack of guidance in the hotend	Additional PTFE tubing
	Extruding onto a solid surface	Starting over holes
Wire breaks	Radius for a 90° change of the wire's direction of movement to small	Layer height of 0.6 mm
	Discrepancy between travelled length and length of deposited wire	Minimum radius of 5 mm with a printing speed of 1 mm/s

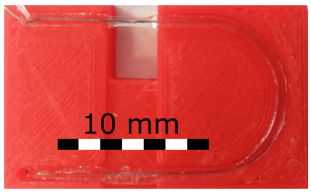

FIGURE 5. Printed specimen for the evaluation of the performance of used hybrid filament variants.

With the standard printing parameters, a flow rate of 4.8 mm^3/s is generated through the nozzle. The hybrid filaments have different flow rates assuming a printing speed of 10 mm/s (F12: 10.5 mm^3/s; F10: 8.4 mm^3/s; F075: 4.2 mm^3/s; F045: 1.35 mm^3/s). The recommended flow rate for the hotend system used is 7.5 mm^3/s. The increased values of samples F12 and F10 can be compensated by increased temperatures or reduced velocities.

Regarding the deposition process, specimen were printed with a predetermined wire path, printing in cavities, printing on a surface and a bridge, which is displayed in Fig.5. This path consists of a 10 *mm* straight line, a 180° turn with a diameter of 10 *mm* and another 10 *mm* straight line. The path was kept, but the geometry was adjusted for each filament. The printing parameters were changed in terms of printing temperature and printing speed in the process to achieve printable results. The samples were evaluated for condition and position of the wire within the polymer encapsulation.

The process of depositing is defined by the different layer heights of the hybrid path and the remaining printed part. Based on the wire diameter, the usable layer height is necessarily above the commonly used 0.2 *mm* layer height of FFF printers. To reduce the loss of accuracy, different layer heights were chosen between the hybrid filament lines and the normal filament lines. As it is not possible under these circumstances to interrupt the printing process, print a hybrid path on the partially printed object and then continue with the construction of the part, as the next layers would collide with the hybrid lines, it was chosen that the hybrid lines should be deposited in cavities. This is done analogously to the use of conductive pastes. With this method, the hybrid line closes with the top of the printed part and further layers can be added. The filament samples F10 and F12 deviate from the recommended parameters for 0.4 *mm* nozzles due to their layer height. Paths with this height would lead to inaccurate geometries, but due to the surrounding cavity this is not to be considered.

For this process, cavities must be constructed in the form of a path plan in the computational aided design (CAD) used. These are rectangular with the layer height and line width to be filled with the hybrid line. In addition to the cavities, starting points were also constructed in CAD to serve as fixed points for the end of the wire. A representation of such a CAD file with the required paths can be seen in Fig.20. During the further printing processes with the hybrid filament, the previously deposited polymer should secure the wire and pull it out of the melt zone when the print head advances. The polymer should reattach to the wire when it is cold enough, securing the process. The starting points are holes through a set of layers into which the hybrid filament can be pushed. The machine code (G-code) required to place the hybrid filament in the planned path, start and end points was not generated from slicing software (such as Slic3r, Cura, S3d, etc.) like the other commands, but implemented manually. For this reason, standardised G-code fragments were prepared. The generation of the actual printed part can be done with any slicer, with any material and with any settings. We used Cura 4.7.0 and did the post-processing of the G-code with Notepad++ v7.5.

B. CUTTING

- fixed parameters:
  - wire diameter 0.2 *mm*;
  - wire material copper;
  - encapsulation material PLA;
  - hybrid filament diameter 1.0 *mm*
- varying parameters:
  - method of cutting

In order to be able to be mounted on different print heads without significant mechanical adjustments in the respective device, the cutting device was designed as an add-on module. Three main section where a cutting can be done, were analysed. Those sections are displayed in Fig.6. The shortest possible length of wire that can be deposited is defined by the distance between the cutter and the nozzle tip. When cutting in the first section (1), between the extruder and the hotend, additional resistance and thus higher required forces must be expected, as the solid polymer must be cut through. This leads to higher demands on the kinematics or the actuator. If the separation takes place in the second section (2), within the heating block where the polymer is melted, the heating block must be reconstructed, which leads to increased modifications and a complex heating block. Considering these

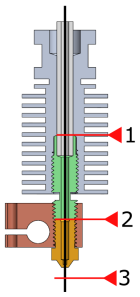

FIGURE 6. Positions to possibly cut the continuous wire inside the used Hotend system(1- between Extruder and Hotend, in cold state; 2- Inside the melting zone 3- after the nozzle).

conditions, we decided to cut in the third section (3), below the nozzle. This means that the hotend does not have to be modified, only the cutter has to be lifted above the nozzle during printing movements.

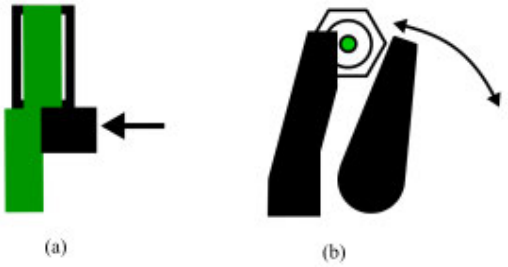

FIGURE 7. Chosen cutting Methods (a) Shearing the hybrid filament at the tip of the nozzle (b) blade cutting the Filament beneath the nozzle.

To achieve this, two separation methods have been chosen for a realization. These methods are shown in Fig.7. Both procedures require a volume beneath the nozzle, in which the cutting can be conducted. Accordingly, this means that the print head must be lifted off the current layer. During this move, a corresponding length of hybrid filament is extruded. Due to both separation methods, a hybrid line remains which is perpendicular to the part surface. This residue is subsequently smoothed into the current layer, to avoid collision with following layers. In 3D printing, such a process is called ironing. To accumulate with the additional material, a notch was provided within the CAD at the end of the hybrid path.

To keep the components used for the module small and lightweight, servo motors (SH-0255MG from Savox) are used to actuate the cutting device. For the desired application, up to two servo motors must be controlled, as a cutting and a lifting movement is required. Although various 3D printer mainboards offer the possibility to connect servo motors to selected pins, this is not generally available. Therefore, the control of the actuators was outsourced from the mainboard and the required code and wiring was done via a daughterboard. For this purpose, an Arduino nano ATmega 328 was wired to pin80, an unused pin of the expansion header of the gtr v1.0 mainboard. The wiring of the Arduino nano is shown

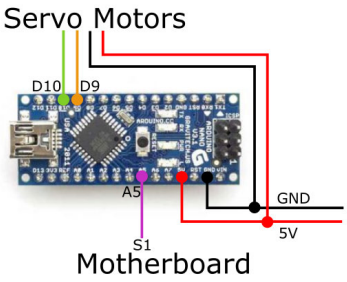

FIGURE 8. Schematic of the wiring used to control the servos, that actuate the cutting mechanics.

in Fig.8. Alternatively, any PWM (Pulse Width Modulation) pin could be used. The Arduino receives a start signal from the motherboard with the G-code command M42 P80 S0-255 to execute the desired motion sequence. Thus, the control of the servo motors is triggered by a required G-code command. This allows the wire cutter to be used with any firmware and any electronics.

C. CONTACTING

- fixed parameters:
  - wire diameter 0.2 *mm*;
  - encapsulation material PLA;
  - hybrid filament diameter 1.0 *mm*
- varying parameters
  - insertion length;
  - insertion temperature;
  - insertion speed;
  - contacting method;
  - contact geometry

The method chosen for depositing the wire provides that wire and polymer can only be extruded simultaneously. Accordingly, the wire is encapsulated at every moment of deposition. Due to this constraint, the wire must be exposed before contacting is possible. This partial process must not damage either the polymer substrate or the wire. Since the hybrid line with its copper core is considered a single unit, mechanical, chemical and thermal stripping processes were investigated. Since the process is to be carried out by the printer itself and both the thermoplastic as encapsulation material and the printer with its heated print head meet the requirements for a thermal stripping process, this method is favoured.

Two concepts were developed in which the embedded wires are contacted one after the other by thermal inserts. Variant 1 provides for a subsequent electrical connection via a screw - variant 2 via a soldered or plug-in connection. Both have solid contact elements that are thermally pressed into the polymer part. In this way, the contact elements are used both for stripping the wire from the surrounding polymer and for contacting in a combined work step. The first concept is based on contacting conductive layers within fibre composites by riveted joints [29], [30], through a conical metal insert and will further addressed as Method C1.

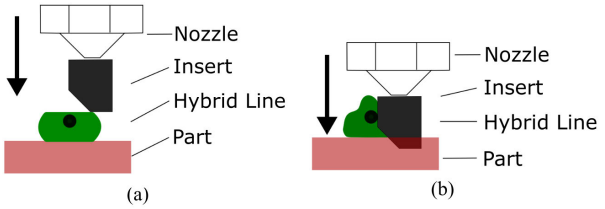

FIGURE 9. Method C1 for Contacting embedded wires through displacement with a conical shaped insert (a) insert is positioned on the part (b) the insert is heated and pressed into the polymer layers. The wire is dislocated form the original position and forms a line contact with the insert.

The wire is displaced from its original path by a conically shaped metal insert. This forms a line contact between the wire and the contact element. This process is illustrated in Fig.9. To achieve this purpose, brass threaded inserts are used, which are already known as post-processing for printed parts. These inserts were sanded to give them a 45° chamfer on one side. The second concept is based on a clamping contact and is addressed as method C2. Here, a metal plate is heated and pressed onto the hybrid line. The local temperature rise is used to widen the polymer line until the wire is exposed. The metal plate forms a line contact with the wire. This method is shown in Fig.10. For the thermally pressed contact plates, 5.0 x 5.0 x 0.5 *mm* square copper sheets were used, as a basic shape.

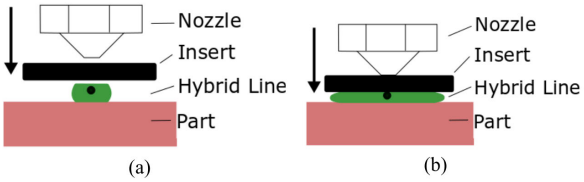

FIGURE 10. Method C2 for contacting embedded wires with a contact plate (a) insert is positioned on the part (b) the insert is heated and pressed into the polymer layers. The polymer is widened and the wire forms a line contact with the insert.

Contacting takes place after the wire embedding sequence is completed. The printing process is stopped, a wire path is laid into the cavities and the wire is separated from the hot end. The user then places the contact elements on the part at the designed contacting positions. The printer then performs the thermal placement and the printing process continues. To achieve the highest possible serviceability, the following conditions must be covered by the contacting methods.

- 1. Interlayer contact (through different layers)
- 2. Intralayer contact (within the same layer)
- 3. external contacting possibilities (stressable, ideally detachable)

Interlayer contacts are used to create connections perpendicular to the plane in which the wire is embedded. This is needed to connect different paths in separate layers within the component. Furthermore, intralayer contacts are needed to connect paths within the same layer, if necessary. And finally, the contacting methods must be suitable to connect to electronics outside the component.

After depositing the hybrid path and then generating the required polymer structures, the contact element was manually placed on the component. Subsequently, the position of the thermal insert was automatically approached with the print head. For the contacting of the wire with the insert or the integration of the contact element into the component, the element is heated to a polymer-specific target temperature.

For the use of PLA as matrix material, the nozzle temperature was set to 210°C and the threaded insert was approached for 8 seconds. The insert was then moved 2.6 *mm* at a speed of 10 *mm*/*min*. For the metal plates, the nozzle temperature was set to 220°C due to the smaller contact area with the nozzle and pushed 0.6 *mm* at the same speed as above. In method C1, the threaded inserts, the nozzle touches the insert with its collar. This causes the insert to be aligned perpendicular to the surface and centred on the nozzle. With method C2, the metal plates are only touched by the tip of the nozzle. The contact area is therefore dependent on the nozzle size used. There is no alignment by the nozzle. When placing the component down, the positioning of the contact plates must be secured manually. Due to the heating during thermal pressing, the inserts close flush with the upper layer of the printed object. The generative process is then continued.

In both methods, the manufactured test specimen should have a fully embedded wire and two contact elements that are connected to each other via this wire. This results in a test specimen with two external contact points that are conductively connected to each other. In the case of the threaded inserts (method C1), these were inserted centred in a wire loop (see Fig.16(a)), in order to achieve the longest possible line contact between insert and wire. The contact plates (method C2) were used in straight passages as there is no difference in the length of the line contact due to placement. For the measurements, test pieces were made that feature an upper and a lower contact plate twice, connected by an embedded wire. Therefore, both the upper and the lower plate are accessible from the outside (see Fig.20(b)).

After successfully performing both contacting methods, the contact resistances were measured to validate the contact quality of both methods. This contact quality is specific to the printer system and must be individually adjusted for other devices. Only a small sample quantity is measured in order to obtain a qualitative statement about the contact quality, as no parameter studies could be carried out on different machines so far. For threaded inserts, test specimens were constructed for inserts of sizes M4 to M6, each with three configurations of wire spacing. Each of these models was printed three times. The test specimen for the contact plates has external contacts on the upper and lower plates to evaluate differences in plate position. Fifteen test specimens were made for this purpose. The test specimens were measured with the circuit shown in Fig.11. The measurement is conducted using the four-wire method with the SRM-05 (Elabo) instrument for small resistances on probes that were consecutively manufactured.

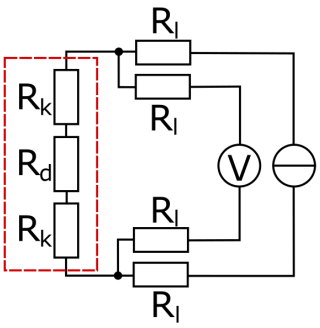

FIGURE 11. Schematic of the used structure to measure the contact resistance of the printed probes using the four wires measure method (R_k - Contact resistance, R_d - wire resistance, R_l - cable resistance).

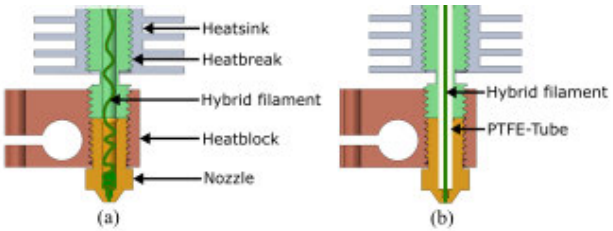

FIGURE 12. Clogging inside the print head caused by the hybrid filament not being guided (a). PTFE adapter tube (white) inserted in the original filament path to compensate the thinner hybrid filament (b).

III. RESULTS

A. PRINTING RESULTS

Extrusion problems were observed when guiding the hybrid filament inside the hotend. Repeated clogging of the nozzle was observed. This clogging is caused by the wire not exiting the nozzle but deforming within the feed path (see Fig.12(a)). Two causes were identified. First and foremost, the thinner F045 and F075 filaments (relative to 1.75 *mm* filament) lacked guidance within the hotend system. The pressure temperatures inside the heating block caused all the hybrid filaments used to deform as they were pushed through the nozzle. This caused the wire to block the nozzle and build up inside the hotend.

Secondary blockages were observed when the hybrid filament was extruded onto a solid surface. In this way, the wire did not change its direction of movement and built up inside the heating block without extruding. To address these observations, an additional PTFE inliner was placed in the feed path (see Fig.12(b)). Teflon tubing is commonly used to guide filaments inside heating blocks. The chosen piece of tubing had an outer diameter of 2 *mm* and inner diameter corresponding to the hybrid filament used. In this way, it can be used as an adapter to reduce the diameter of the feed paths of different hotends without changing the mechanical parts. This adaptation has improved the guidance and prevented the main cause of clogging. In the secondary cause of clogging, the PTFE hose in the nozzle area was damaged and had to be replaced.

Filament sample F045 showed increased cases of clogging inside the hotend despite the PTFE adapter. It was not possible to deposit the wire reliably. The thinnest filament probe was too unstable to be extruded with the conventional components. The same observation could be made with the test piece F075, but attenuated. Regarding the feeding process, samples F10 and F12 showed no differences to the conventional filaments. When depositing the wire on an underlying printed part, the F075 hybrid filament and the used layer height of 0.4 *mm* were problematic. The small given radius for a 90° change of the wire's direction of movement in combination with the sharp corner of the nozzle exit led to wire breaks.

These breaks usually lead to blockages. No differences in performance could be found between the F10 and F12 filaments in the printed specimen. Both filaments give good results when placed in a cavity, freely on a surface or over a clearance. The line width behaves as expected. It was decided that the F10 specimen would be used for all subsequent tests, as the cross-section is smaller than that of the F12 variant. The chosen parameters with a layer height of 0.6 *mm* are advantageous in combination with the other generation of the component, as the hybrid layer height is a multiple of the usually used layer heights (0.1 *mm*; 0.15 *mm*; 0.2 *mm*; 0.3 *mm*). In this way, there is no overlap due to the use of these layer heights. The cavities are completely filled with the hybrid path. The pressure parameters used resulted in good flowability of the substrate material. Despite the high flow rate, there are no delamination phenomena. Due to the slow printing speeds, there is an increase in temperature in the polymer environment. This is theoretically beneficial for the layer bond. The printed hybrid paths cannot be separated from the surrounding component.

The position of the wire in straight passes is centred within the hybrid line. The wire is located in the upper half of the polymer encapsulation and is completely surrounded by the thermoplastic, as can be seen in cross-sections (see Fig.13(a)). During curves the wire is displaced from the middle position (see Fig.13(b)), towards the inner diameter of the circular path (see Fig.13(c)). This observation is analogue to observations during the FEAM wire deposition process [24]. The central alignment is ensured by the nozzle diameter. Larger nozzle diameters showed worse repeatabilities.

If the radii used for the changes of direction are too small, the discrepancy between the length travelled and the actual length of wire deposited becomes too great and wire breaks occur (see Fig.13(d)). Experiments have shown that sudden changes in the direction of movement cannot be used without a circular path, as they lead to an immediate displacement of the wire. This in turn leads to blockages in the hotend, resulting in a failure of the print. As suspected, the previously deposited hybrid line acts as a retainer for the wire as the cooled polymer provides a holding force. When the direction of movement is changed, the wire is displaced as the freshly printed line does not provide a holding force. It was observed that slow printing movements, at 1 mm/s, lead to smaller displacements in the curves than higher speeds. Therefore, the traverse speed for circular movements was set to 1 mm/s

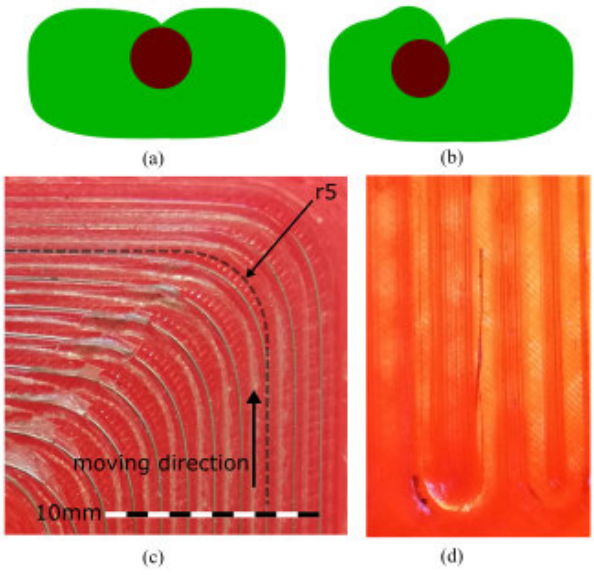

FIGURE 13. Schematic cross-section of the hybrid line on straight paths (a). Schematic cross-section of the hybrid line in curves (b). Displacement of the wire in 5 *mm* curves at 1 *mm/s* (c). Wire break after a 180° turn with 2.5 *mm* radius (d).

to allow for the greatest possible cooling. On straight passages, printing speeds of 10 *mm/s* could be run safely without a decrease in process quality being observed. We assume that the temperature influence, the cooling behaviour and the curve diameter are critical parameters for a successful process. After performing meander tests (as shown in Fig.13(b)), we suggest a minimum radius of 5 *mm* for the given pressure parameters to achieve the best reliability.

In the tests carried out with hybrid filaments (approx. 100h printing time), no abrasive influences on the brass nozzle used could be detected.

B. CUTTING

1) SHEARING

In the first approach, a shearing process was realised that separates the wire at the exit of the nozzle. For this purpose, a mechanism was successfully developed that couples the cutting with the movement below the nozzle (see Fig.14). In this way, only one servo motor was needed to actuate the process and the device can therefore be simple. This was achieved by mounting the cutter used rotatably on the heating block. The rotation allows moving the blade above the nozzle during the printing movements and an almost linear shearing process at the nozzle exit. This process was achieved by a four-linkage coupling drive, which was coupled to the servo motor. The servo motor in turn was mounted on the print head. The blade was fixed to the heating block by means of an additional hole on the side of the heating block, into which a pin was inserted. In case of an adaptation for different hotends following this construction, this part has to be exchanged. An advantage is that by tightening the nozzle, an exact adjustment of the nozzle tip in relation to the blade can be made.

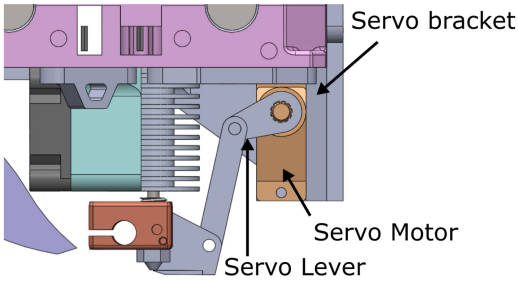

FIGURE 14. Implementation of the shearing mechanism.

The realisation of this approach results in a small additional weight of about 65 g, which is added to the print head. The control via the four-linkage couple drive allows a relatively free positioning of the servo motor. In the configuration used, a rotation of 60° was required to cut the wire. The actuator used applies a torque of 39 Ncm, which was sufficient to repeatedly cut the specified 0.2 *mm* copper wire. It was found that during the printing process, the parts mounted on the heating block were heated to the target nozzle temperature.

2) BLADE CUTTING

The second approach was intended to be independent of the hotend system used. This was achieved by decoupling the moving and cutting processes. The cutting process is based on a blade cut with a counterpart. The cutter is moved by a linear guide below the nozzle. This movement uses a 30° angle for centring under the nozzle tip. This allows different hotend systems to be used without any problems if a corresponding receptacle for the print head is available. The movement device and the cutting device are each driven by a servo motor. With this module, a residual length of 3 *mm* of Hybird filament could be detected below the nozzle after the cutting process. For this reason, a retract command was implemented after the cutting sequence so that the wire would not collide with the subsequent layers. In this way, the further generation of the part could take place without any influences. When retracting the wire, no negative influences on the process could be observed. It was found that a small amount of polymer was lost from the hybrid line during this process, as it was not retracted into the nozzle. This was compensated by the used starting point of the respective hybrid line, as the wire is pushed into the component.

The realisation of the knife cutting concept resulted in a module with an additional weight of 95 g at the print head. the downward movement, can be adjusted separately from the cutting movement. Due to the decoupling from the hotend, no process influence was observed with regard to the thermal properties and the specified printing process.

C. CONTACTING

1) THREADED INSERTS

As mentioned in the before, the threaded inserts are used in the center of a wire loop (see Fig.16(a)). Here, the

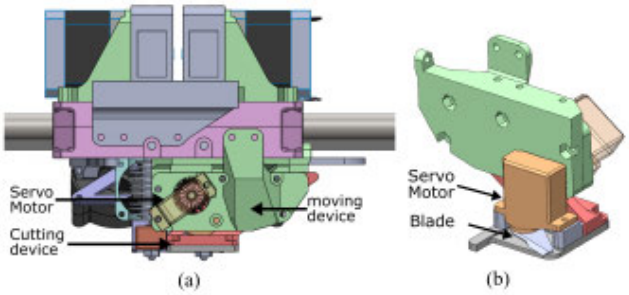

FIGURE 15. Implementation of the blade cutting mechanism (a) Module fitted on the print head (b) isolated display of the Cutting module from behind.

FIGURE 16. Method for Contacting embedded wires through displacement with a conical shaped insert (a) printed structure with a wire path forming a ring, in which the threaded insert is pressed in (b) damaged wire after removing the insert to inspect the contact geometry.

displacement of the wire in curves led to a negative process result. The desired position in relation to the thread insert could not be achieved. The conical insert did not displace the wire as intended and wire breaks occurred (see Fig.16(b)). For this reason, it was determined to place the contacting point in straight segments, thus achieving a higher accuracy of the wire position.

In addition, this results in the possibility of performing intra-layer contacts between parallel wires. In further trials, it was found that the polymer displaced by the threaded insert interferes with the process of exposing the wire. The downward movement of the insert pushes the filament against and over the wire. This leads to a displacement of the wire in the Z-direction and thus to a failure in exposing the wire. Therefore, the contact geometry of the printed part was optimised so that there is as little additional polymer as possible in the area of the contact. The altered process (opposed to Fig.7) of using the threaded inserts is shown in Fig.17. Under the given circumstances, test specimen were successfully manufactured with M4, M5 and M6 sizes of threaded inserts. The used configurations are displayed in Fig.20(a). These test specimens contain two inserts that contact two parallel embedded wires. In this way they form a conductive connection. During the production of these parts, it was found that reliable contacting of the wires could not be realised with the use of M4 inserts. The small chamfer provided by the M4 taper was not sufficient to reliably move the wires. Therefore, no further tests were carried out with the M4 configuration of the printed specimen. In addition to

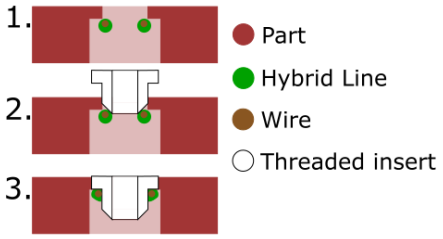

FIGURE 17. Improved process to use the threaded inserts to contact the embedded wires (1 - Insert is placed in the printed object, 2 - Insert is heated through the contact with the nozzle, 3 - Insert is pushed into the part to displace the wire).

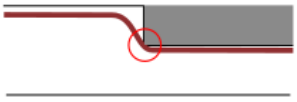

FIGURE 18. After the contact plate is pressed onto the hybrid line, the wire is pressed into the layers beneath. Only a point contact is acquired and the marked position.

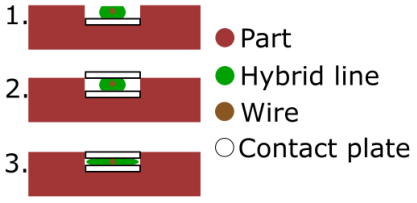

FIGURE 19. Improved process to use the contact plates to contact the embedded wires (1 - hybrid line is laid onto a contact plate, another is placed on top, 2 - the upper plate is heated through contact with the nozzle, 3 - the plate is pressed onto the hybrid line to deform the encapsulating polymer).

intra-layer contacting, inter-layer contacts could also be made by depositing several hybrid lines on top of each other and connecting them with a threaded insert.

2) CONTACT PLATES

In method C2, it was observed that pressing a plate onto the hybrid line was not sufficient to achieve stable contact. The wire was not exposed as planned, but pressed into the underlying polymer layer. In this way, only a point contact was formed, as shown in Fig.18. To circumvent this behaviour and achieve line contact, the method was changed. From now on, two contact plates are used, one below the hybrid line and one above the line. This change is shown in Fig.19. This requires an additional step in the placement of contact elements before and after the deposition of the hybrid line. After embedding the wire, the upper plate is placed on the printed part and pressed into the hybrid line. In this way, the wire is clamped between the contact plates and both are conductively connected. The modified process showed a significantly better performance of the contacting method in terms of repeatability. For the production of intralayer

connections, two parallel hybrid lines could be connected, using one contact plate for both. When soldering the contacts, it was observed that the subsequent high temperature severely damaged the contact points, as they were destroyed in most cases. The occurring temperature causes a deformation of the surrounding polymer and thus a displacement of the wire. As a first alternative, pre-soldered contact plates were used in the test objects. In other test objects, simple plug connections were realised. In addition to the intralayer connections presented, interlayer connections were also made in which the contact plates were stacked through several layers of the component.

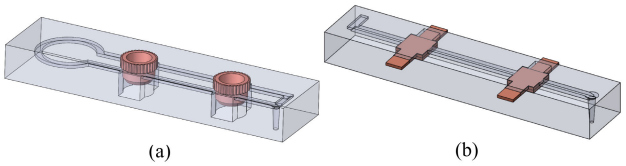

FIGURE 20. CAD visualization of the test parts for measuring the contact resistances, geometry for threaded inserts (a), geometry for contact plates (b).

3) CONTACT RESISTANCE

The final specimen which were manufactured for both methods are displayed in Fig.20. The resistance of the wire between the contact elements ((a): 0,0054 Ω; (b): 0,0087 Ω) was subtracted from the measured value. During the usage of the contact plates, it was observed that the upper plate generally shows a lower contact resistance, with less fluctuation, as shown in Tab.3. This corresponds to the wire position in the upper part of the hybrid line.

TABLE 3. Average resistance of the contact plates (upper and lower) in 14 specimen.

plate Position	contact resistance in Ω	max. deviation in Ω
upper plate	0.0605	0.0522
lower plate	0.2453	0.0878

The measurements of the threaded insert showed that the contact resistance was related to the distance between the wires of the samples of the three different configurations made for each insert size. It was observed that a higher distance resulted in lower resulting resistances, as seen in Tab.4 In addition, the test specimen with the smallest wire spacing (M5: 5.0 *mm* / M6: 6.0 *mm*) could not produce functional transitions. As before, the insert partially damaged the wire or did not displace it in the desired direction.

The minimum value was achieved with the largest distance between the embedded wires. Additionally, the process reliability was better with larger distances. The best configurations of the threaded inserts for M6 (6.4 *mm* wire spacing) and M5 (5.4 *mm* wire spacing) were each averaged over the three test specimens used and are shown with the average value of

TABLE 4. Average resistance of threaded inserts with different wire distances.

insert size	wire distance in mm	contact resistance in Ω
M5	5.0	/
	5.2	0.0325
	5.4	0.0092
M6	6.0	/
	6.2	0.1577
	6.4	0.0359

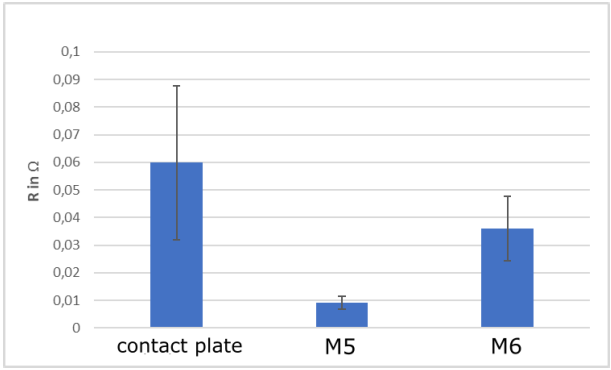

FIGURE 21. Best resulting contact resistance measurements of the used contact methods with a 50% confidence interval.

the upper contact plate contacts (14 test specimens) in Fig.21. Within the experiments conducted, with the parameters used, the M5 inserts with a wire spacing of 5.4 *mm* achieved the lowest contact resistance and the smallest deviation. The resistance obtained is less than 0.01 Ω.

IV. DISCUSSION AND CONCLUSION

In the research work presented, a hybrid filament made of a polymer-encapsulated wire was successfully deposited with a commercially available desktop 3D printer, cut to length and automatically contacted. This enabled the production of additively manufactured parts with integrated conductive paths. Achieving the goal of developing a process to produce additively manufactured parts with integrated conductive traces using consumer-grade printers with minor modifications can be rated as very good. The use of hybrid wire polymer filaments makes it possible to embed conductive traces on low-cost FFF machines. The only modification required for reliable use of the F10 hybrid filament is an additional PTFE tube inside the hotend, which serves as an adapter. In this way, even machines with only one hotend can selectively place wires during article printing when the filament is changed. In multi-material printers, integration can be automatic by using one tool exclusively for the hybrid filament. In single tool 3D printers, wires can be selectively embedded by switching between regular and hybrid filament during printing. The diameter of the embedded wires is higher than with comparable processes [12], [21], [17].

With larger nozzles and adapted parameters, even higher wire diameters could possibly be embedded. Unlike the use

of conductive filaments, no abrasive influences on the nozzle geometry have been observed so far. As expected, rapid cooling of the hybrid line is a criterion for process reliability, as the cured polymer fixes the wire in position. Therefore, the printing parameters must take this into account and slow speeds at low nozzle temperatures should be preferred. For example, the specification of 5 *mm* radii for directional changes limits the usable wire paths. Further developments should focus on reducing this value. Moreover, since the wire does not deform and the polymer adheres to it, the bridging results were very good. To enable a fully automated process, additional technologies for cutting the wire and contacting the embedded structures are needed and have been developed.

The cutting methods also showed positive results. Both approaches were able to safely cut the copper wire used. Other materials, such as steel wires or shape memory alloys, may require revision of the cutting methods due to increased material hardness. Controlling both cutting mechanisms, as done by the Arduino daughterboard, allows the use of a wide range of printer electronics. Cutting can be initiated by setting a pin state of the motherboard via the appropriate G-code command. Even though the G-code generation for the composite parts was done manually, this provides the basis for a full automation of the whole process by software in the context of this research. It is therefore recommended that an extension to the slicer software be developed soon to increase usability and lower the barrier to entry. Further developments should be made in terms of process optimisation and the design of the motion mechanism to obtain a compact and fast-acting slicing module. The shearing process is a simple approach with few, lightweight parts. The servo motor can be positioned quite freely, which is an advantage for implementation on other print heads. At the same time, fixing the cutter to the heating block forces changes to the hotend used. In addition, the lower part of the cutter is heated to the target temperature of the hotend by direct contact with the heater. This leads to a significant increase in the thermal inertia of the hotend system and thus to an increased heating and cooling time. This can potentially affect the printing process, although no negative influences have been observed.

For further development, the knife cutting process is favoured as no such influence is possible here. In addition, the separate movements of cutting and extending can be adjusted depending on the hotend. Due to the independence from the used hotend parts, an adaptation to further machines is possible. The driving and cutting device can form a compact module if the mechanism geometry is further optimised. Therefore, further development should consider reducing the size of the module and designing adapter plates for the most commonly used desktop printers.

The described approach to contacting led to two methods that use thermal inserts. On this basis, the heater cartridges of the hotend are used. Thus, only the placement of the contact elements requires manual intervention, so the contacting is done by the printer. In the additive manufacturing process, these two concepts can be used without changing the mechanics of the printer. The use of conically ground threaded inserts (C1) or copper plates (C2) for the process of contacting embedded wires can be evaluated as good. The evaluation of the contact resistances only provides a limited and qualitative estimate of the achievable resistance values. This is due to the small bandwidth of the samples used. In addition, the only parameter that was changed during the tests is the distance between the wires of the threaded insert samples.

Regarding the contact resistances of both approaches, the contact plates were found to give higher resistances with a significantly higher variation of $0.059 \pm 0.028\ \Omega$ (50% confidence interval). Furthermore, it was observed that the upper plate gives a contact with lower resistance. This could be related to the wire position in the upper part of the hybrid line. The threaded inserts showed differences between the size of the insert and the distance between the contacted wires. The best value was observed when using M5 inserts with 5.4 *mm* distance between the wires, with $0.009 \pm 0.0023\ \Omega$(50% confidence distance). These values are in the order of magnitude of similar approaches such as the riveted joints for fibre composites with 0.01 Ω. [29] or the use of ECPC for FEAM with 0.02 Ω [21]. The threaded inserts give better results in terms of resistance and deviation. This may be related to the centring process by the nozzle and the part geometry, which only occurs with the threaded inserts and not with the contact plates. The use of contact plates reduces the space required for contacting within the part and increases design freedom, as the shape is not relevant to the contacting process. Thus, unlike threaded inserts, which can only be contacted in the Z direction, contact plates can form external contacts in the X/Y/Z direction. Optimisation for the contacting process has not yet been done. Better results can be achieved through experiments on the influence of individual process parameters, such as the insertion temperature, the insertion speed, the contact geometry or the wire position. These parameters should influence the process as they determine the exposure of the wire and the interference with the surrounding polymer. Possible improvements should focus on repeatability and reducing resistance deviation. At this stage, the contact quality is not sufficient to be used for measurement without further control, as the variation in contact resistance is too high, but can already be used for power transmission.

The applications for this novel technology do not have to be limited to the integration of conductive structures. The materials of the embedded wire and the surrounding polymer can be chosen according to the desired characteristics. In addition to copper wires, functional fibres could also be integrated as sensor or heating wires. This would allow sensors or heating elements [18] to be incorporated directly into the end-use parts without further manufacturing. In particular, locally implemented thermal actuators enable new approaches in the field of thermoplastics. Through the integrated wire, the parts can be selectively heated, thereby locally reaching temperatures above the glass transition temperature. This leads to a rubber-like state of the polymer, which allows large

deformations without damaging the structure. In this way, 3D-printed parts can be reversibly formed in a controlled manner after they have been produced. [31].

FIGURE 22. Completely printed model to demonstrate the possibilities of thermal reforming 3D printed structures, a mesh surface with integrated wires (a) printing orientation (b) resulting deformation, after a current was applied and the surface was moved.

Using a simple demonstrator, the integration process of conductive structures was validated with the methods presented. The part has embedded contact elements that form a socket contact for an electrical connector with the surrounding native polymer. The wire is embedded in the horizontal lines of the grid surface. An applied power of 15 W for 90 s causes a phase change in the material near the wire. Since this temperature only affects selected parts of the model, the part softens locally. In the heated state, the structure can be deformed with small forces, resulting in different deformation states, which are held without further energy after the corresponding cooling. This demonstrator is shown in Fig.22. This leads to the assumption that the maximum currents that can be carried within the printed components are determined by the thermal characteristics of the substrate. Under permanent higher loads, the mechanical load capacity of the component is impaired. No measurements have been carried out on this process so far, but this will be aimed for in the future. In summary, it can be stated that the intended development could be successfully realised with three sub-processes. This research provides a contribution to the expansion of the broad field of industrial or private uses of FFF technology without the need for new machines. Despite additional optimisation work, this can be a further step towards enabling decentralised production of highly complex end-use parts.

REFERENCES

[1] (2020). *Additive Fertigung: Branchentrends und-Prognosen*. Accessed: Oct. 1, 2020. [Online]. Available: https://formlabs.com/de/blog/additive-fertigung/#Kompakt
[2] *Trends in 3D Printing at Scale: A Survey of 3D Printing Stakeholders in Production Manufacturing*, Dimensional Res., Sunnyvale, CA, USA, 2020.
[3] J. Crabtree and S. Dunham, "The additive manufacturing landscape 2020—AMFG," in *Proc. Additive Manuf. Landscape*, vol. 2, 2020, pp. 11–17.
[4] U. Petschow, J.-P. Ferdinand, S. Dickel, H. Flämig, and M. Steinfeldt, *Dezentrale Produktion, 3DDruck und Nachhaltigkeit: Trajektorien und Potenziale innovativer Wertschöpfungsmuster zwischen Maker-Bewegung und Industrie 4.0*, vol. 206. Berlin, Germany: Institut für ökologischeWirtschaftsforschung, 2014.
[5] D. Zindani and K. Kumar, "An insight into additive manufacturing of fiber reinforced polymer composite," *Int. J. Lightweight Mater. Manuf.*, vol. 2, no. 4, pp. 267–278, Dec. 2019, doi: 10.1016/j.ijlmm.2019.08.004.
[6] J. Rhys, "Additive manufacturing of functional engineering components," M.S. thesis, Dept. Mech. Eng., Univ. Bath, Bath, U.K., 2013.
[7] M. Hedges and A. B. Marin, "3D aerosol jet printing—Adding electronics functionality to RP/RM," in *Proc. DDMC Conf.*, vol. 1. Albuquerque, NM, USA: Optomec, Mar. 2012.
[8] F. Vogeler, W. Verheecke, A. Voet, and H. Valkenaers, "An initial study of aerosol jet printed interconnections on extrusion-based 3D-printed substrates," *Strojniški Vestnik-J. Mech. Eng.*, vol. 59, no. 11, pp. 689–696, Nov. 2013, doi: 10.5545/sv-jme.2013.999.
[9] K. Gnanasekaran, T. Heijmans, S. van Bennekom, H. Woldhuis, S. Wijnia, G. de With, and H. Friedrich, "3D printing of CNT- and graphene-based conductive polymer nanocomposites by fused deposition modeling," *Appl. Mater. Today*, vol. 9, pp. 21–28, Dec. 2017, doi: 10.1016/j.apmt.2017.04.003.
[10] S. W. Kwok, K. H. H. Goh, Z. D. Tan, S. T. M. Tan, W. W. Tjiu, J. Y. Soh, Z. J. G. Ng, Y. Z. Chan, H. K. Hui, and K. E. J. Goh, "Electrically conductive filament for 3D-printed circuits and sensors," *Appl. Mater. Today*, vol. 9, pp. 167–175, Dec. 2017, doi: 10.1016/j.apmt.2017.07.001.
[11] S. J. Leigh, R. J. Bradley, C. P. Purssell, D. R. Billson, and D. A. Hutchins, "A simple, low-cost conductive composite material for 3D printing of electronic sensors," *PLoS ONE*, vol. 7, no. 11, Nov. 2012, Art. no. e49365, doi: 10.1371/journal.pone.0049365.
[12] D. Espalin, D. W. Muse, E. MacDonald, and R. B. Wicker, "3D printing multifunctionality: Structures with electronics," *Int. J. Adv. Manuf. Technol.*, vol. 72, nos. 5–8, pp. 963–978, May 2014, doi: 10.1007/s00170-014-5717-7.
[13] A. Cohen *et al.*, "Methods for fiber reinforced additive manufacturing," WO Patent 2014/197 732 A2, Apr. 9, 2019.
[14] G. T. Mark and A. S. Gozdz, "Apparatus for fiber reinforced additive manufacturing," U.S. Patent 2014 0 328 963 A1, Mar. 22, 2013.
[15] A. V. Azarov, M. V. Golubev, F. K. Antonov, and A. R. Khaziev, "Print head for additive manufacturing of articles," EP Patent 3 611 007 A1, Oct. 4, 2017.
[16] A. V. Azarov, V. V. Vasilev, A. F. Razin, and V. A. Salov, "Composite reinforcing thread, preprag, tape for 3D printing and installation for preparing same," EP Patent 3 450 486 A1, Apr. 26, 2016.
[17] Y. Ibrahim, G. W. Melenka, and R. Kempers, "Fabrication and tensile testing of 3D printed continuous wire polymer composites," *Rapid Prototyping J.*, vol. 24, no. 7, pp. 1131–1141, Oct. 2018, doi: 10.1108/RPJ-11-2017-0222.
[18] Y. Ibrahim, "3D printing of continuous wire polymer composite for mechanical and thermal applications," M.S. thesis, York Univ., Toronto, ON, Canada, 2019.
[19] D. Löffler, I. Dani, R. Metke, and M. Knobloch, "Vorrichtung zum dreidimensionalen ab-oder verlegen von mit einer ummantelung versehenen filamenten," DE Patent 10 2019 206 539 A1, Dec. 11, 2020.
[20] A. L. Cohen, P. S. Krueger, M. Saari, E. Richer, B. Cox, B. Xia, and C. G. Clay, "Additive manufacturing of active devices using dielectric, conductive and magnetic materials," U.S. Patent 10 254 499 B1, Aug. 4, 2017.
[21] B. Xia, M. Saari, B. Cox, E. Richer, P. S. Krueger, and A. L. Cohen, "Fiber encapsulation additive manufacturing: Materials for electrical junction fabrication," in *Proc. 26th Annu. Int. Solid Freeform Fabr., 27th Annu. Int. Solid Freeform Fabr. Symp. Additive Manuf. Conf.*, 2016, pp. 1345–1358.
[22] M. Saari *et al.*, "Active device fabrication using fiber encapsulation additive manufacturing," in *3D Printing and Additive Manufacturing*, vol. 2, no. 1. 2015, pp. 26–39.
[23] M. Saari, B. Cox, E. Richer, P. S. Krueger, and A. L. Cohen, "Fiber encapsulation additive manufacturing: An enabling technology for 3D printing of electromechanical devices and robotic components," *3D Printing Additive Manuf.*, vol. 2, no. 1, pp. 32–39, Mar. 2015, doi: 10.1089/3dp.2015.0003.
[24] M. Saari, "Design and control of fiber encapsulation additive manufacturing," Ph.D. dissertation, Univ. Texas, El Paso, El Paso, TX, USA, 2019.
[25] M. Liang, C. Shemelya, E. MacDonald, R. Wicker, and H. Xin, "3-D printed microwave patch antenna via fused deposition method and ultrasonic wire mesh embedding technique," *IEEE Antennas Wireless Propag. Lett.*, vol. 14, pp. 1346–1349, 2015, doi: 10.1109/LAWP.2015.2405054.
[26] C. Shemelya, F. Cedillos, E. Aguilera, D. Espalin, D. Muse, R. Wicker, and E. MacDonald, "Encapsulated copper wire and copper mesh capacitive sensing for 3-D printing applications," *IEEE Sensors J.*, vol. 15, no. 2, pp. 1280–1286, Feb. 2015, doi: 10.1109/JSEN.2014.2356973.
[27] J. Owen. (2015). *Enabling R&D—Thermo-Forming Trials*. Accessed: Oct. 1, 2021. [Online]. Available: https://enablingthefuture.org/2015/05/04/enabling-rd-thermo-forming-trials/

[28] German RepRap. (2016). *X350 3D-Drucker Anleitung*. Accessed: Oct. 1, 2021. [Online]. Available: https://bit.ly/2O2GOod
[29] W. Hufenbach *et al.*, "Experimental investigation of combinded electrical and mechanical joints for thermoplastics composites," Ph.D. dissertation, Inst. Lightweight Eng. Polym. Technol., TU Dresden, Dresden, Germany.
[30] W. Hufenbach, F. Adam, A. Winkler, D. Weck, and R. Kupfer, "Integration and evaluation of mechanical and electrical joints in function integrative textile reinforced thermoplastic composites," in *Proc. 15th Eur. Conf. Compos. Mater.*, Venice, Italy, vol. 15, 2012, pp. 1–8.
[31] K. Mäntyjärvi, T. Iso-Junno, A. Mustakangas, T. Jokelainen, M. Kesktialo, and A. Järvenpää, "Exploitation of forming of the 3D printed materials," Univ. Oulu, Oulu, Finland, Tech. Rep., doi: 10.1007/s00170-015-7973-6.

FABIAN ZIERVOGEL was born in Bad Saarow, Germany. He graduated in mechanical engineer, specialization product development from Technical University Dresden, in 2020. Since 2018, he has been working as a Research Assistant with the Fraunhofer Institute for Machine Tools and Forming Technology, Dresden. His research interests include the development of new applications for additive manufacturing, composite 3D-printing and development of adaptive systems.

LUKAS BOXBERGER was born in 1990. He received the bachelor's degree in 2014. He studied industrial design from the Burg Giebichenstein University of Art and Design Halle and product design from the University of Applied Science Dresden, from 2010 to 2017. He set up the Makerspace at the Saxon State and University Library Dresden (SLUB). Since 2014, he has been researching in user-centered, adaptive products, as a Research Associate with the Fraunhofer Institute for Machine Tools and Forming Technology Dresden. Since 2019, he has been a Group Leader for Smart Structures. His research interests include morphing surfaces, soft robotics and production technologies for multifunctional, and function-integrated structures.

ANDRÉ BUCHT received the M.Sc. degree in electrical engineering from the Dresden University of Applied Sciences (HTW) and adaptronics from the Private University of Applied Sciences Göttingen (PFH). Since 2006, he has been working with the Fraunhofer Institute for Machine Tools and Forming Technology in the field of smart materials and systems. He took over as the Head of the Materials and Components Group, in 2009. He was mainly involved in the development of adaptronic components for automotive and mechanical engineering. Since 2011, he has been responsible for the Adaptronics Department as the Head of the Department.

WELF-GUNTRAM DROSSEL was born in 1967. He studied information technology and technical acoustics from the Technische Universität Dresden. He received the German Diploma degree, in 1992, and the Ph.D. degree in simulation of forming processes from the Institute for Metal Forming, TU Bergakademie Freiberg, in 1998. He worked as a Research Assistant with the Institute for Metal Forming, TU Bergakademie Freiberg. He started at the Fraunhofer-Institute for Machine Tools and Forming Technology – IWU, gained a teaching position at Technische Universität Chemnitz in Machine Tools - Mechatronics, in 2004, became an Associate Professor, in 2006, and was appointed to the full professorship of Adaptronics and Functional Lightweight Design, in 2014. Since 2014, he has been the Director of the Fraunhofer IWU concentrating his research on active materials, adaptronic components, technologies for functional integration as well as additive manufacturing.